2015 International Particle Accelerator Conference, Richmond, VA, May 3rd – 8th, 2015

FEASIBILITY STUDY FOR AN X-RAY FEL OSCILLATOR AT THE LCLS-II*

T. J. Maxwell#, J. Arthur, Y. Ding, W. M. Fawley, J. Frisch, J. Hastings, Z. Huang, J. Krzywinski, G. Marcus, SLAC, Menlo Park, CA 94025, USA
K.-J. Kim, R. R. Lindberg, D. Shu, Y. Shvyd'ko, S. Stoupin, ANL, Argonne, IL 60439, USA

Abstract

We show that a free-electron laser oscillator generating X-ray pulses with hard X-ray wavelengths of order 0.1 nm is feasible using the presently proposed FEL-quality electron beam within the space of existing LCLS-II infrastructure when combined with a low-loss X-ray crystal cavity. In an oscillator configuration driven by the 4 GeV energy electron beam lasing at the fifth harmonic, output x-ray bandwidths as small as a few meV are possible. The delivered average spectral flux is at least two orders of magnitude greater than present synchrotron-based sources with highly stable, coherent pulses of duration 1 ps or less for applications in Mössbauer spectroscopy and inelastic x-ray scattering.

INTRODUCTION

Contemporary light sources based on the X-ray free electron laser such as the LCLS [1] and SACLA [2] utilizing self-amplified spontaneous emission (SASE) are now in operation delivering previously unrealizable per-pulse X-ray brightness enhanced over synchrotrons due to the partial longitudinal coherence and full transverse coherence from the high-gain X-ray amplification of ultra-short pulses. However, due to the stochastic nature of the SASE process, the production of stable, fully coherent X-ray pulses remains a challenge for accelerator-based light source facilities world-wide. Hard X-ray self-seeding (HXRSS) demonstrated improved longitudinal coherence and spectral brightness [3] by reducing the X-ray bandwidth mid-amplification to concentrate downstream gain into a narrower spectrum. While this has led to a 2- to 5-fold increase in brightness, HXRSS still relies on the SASE seed, not reaching full, stable longitudinal coherence.

Since the advent of proposed high-rep rate, superconducting FEL linac drivers such as that of the LCLS-II [4], new potential solutions emerge. In this Manuscript, we revisit one scheme based on the continuous recirculation of X-rays to be used for seeding subsequent shots: the low-gain X-ray FEL oscillator (XFELO) [5]. In an XFELO, a low-loss X-ray cavity is wrapped around the FEL undulator, as in an optical FEL oscillator. Where the beam rep rate is equal to the round-trip time of the cavity and the single-pass, low-gain power increase exceeds the round-trip power loss (to initiate start up), the intra-cavity power builds exponentially over many passes, saturating as the single-pass gain comes to equilibrium with the loss. We consider whether a device satisfying these starting requirements is feasible for an LCLS II-type beam, and with what basic considerations.

LAYOUT

Constructing a low-loss X-ray cavity on a scale sufficient to contain an FEL undulator presents difficult challenges. As a best candidate, we suppose an XFELO geometry using high-reflectivity diamond crystal mirrors in a near-backscattering Bragg geometry [6]. To allow for central energy tunability, we adopt the proposal of [7], as illustrated in Figure 1. The electron beam is injected magnetically into the undulator. Four symmetrically arranged Bragg crystals are used to recirculate the hard X-ray output, with two (or two sets of) compound refractive lenses (CRLs) providing cavity focusing. The first crystal following the undulator would be made thin to allow a 4% out coupling of useful radiation.

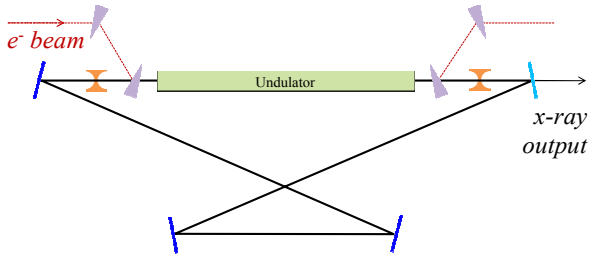

Figure 1: XFELO four crystal, two CRL cavity geometry

The baseline LCLS-II calls for a 4 GeV electron beam energy with variable gap undulators to allow X-ray generation from 0.25 – 5 keV. As the XFELO operates in low-gain, we consider a fifth harmonic XFELO [8] to allow operation well within the hard X-ray regime above 8 keV. At the LCLS-II repetition rate of 0.929 MHz, a round-trip cavity length of 323 m would be required. With the primary restriction of beam rate presumed to be the average beam power on the MW-class primary beam dumps of the ~1 MHz beam at 4 GeV and 100 pC per bunch, we consider doubling the beam rate to 1.86 MHz at a reduced 50 pC per bunch so that the cavity length may be shortened to 161 m.

Under these assumptions, several photon energies are achievable using diamond crystals. In particular, 14.4 keV of the C* (337) reflection, 9.13 keV with C* (333), and

* Work supported under US Department of Energy contract DE-AC02-76SF00515.
# tmaxwell@slac.stanford.edu

13.8 keV using C* (355), present reasonable internal Bragg reflection angles $2\theta_r$ of 18.4°, 17.0°, and 29.3°, respectively. With a 161 m round-trip length, such a cavity would fit within the footprint of SLAC's 62 m x 37.5 m End Station A (ESA), as shown in Figure 2, which includes an existing MW-class beam dump. To avoid the dispersion suggested in the sketch of Figure 1, a double bend achromat can be used to inject the beam into the XFELO undulator, with X-ray delivery either in the SLAC research yard or beyond the subsequent hill to LCLS experimental halls.

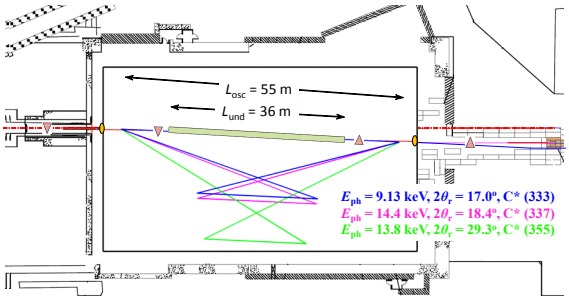

Figure 2: Scale drawing of a tunable XFELO in the SLAC ESA for two photon energies

Using this geometry, LCLS II-typical XFELO beam parameters are listed in Table 1. We consider a 32.5 m magnetic undulator length of the suggested 36 m actual length shown in Figure 2 and mid-undulator Rayleigh length of 6.5 m which can be provided by 21 m focal length CRLs (or CRL combinations) at 14.4 keV. Further assuming 6D Gaussian beam and photon distributions, we apply the low-gain formalism presented in [9] to arrive, after careful integration, to a gain of 40.8%, per pass.

Table 1: Fifth harmonic XFELO parameters

Parameter	Value	Units
e^- beam energy	4.0	GeV
Photon energy @ 5th harmonic	14.4	keV
Peak current	120	A
Bunch charge	50	pC
Bunch length (FWHM)	416	fs
Energy spread (RMS)	200	keV
Norm. emittance	0.3	μm
N undulator periods	1250	
Und. length w/ λ_u = 26 mm	32.5	m
K	1.433	
β_x	10.5	m
$z_{Rayleigh}$	6.5	m
Est. gain per pass	40.8	%

Beam Transport to ESA

Transporting the beam to ESA requires navigating the bends of SLAC's Beam Switch Yard (BSY) while preserving the low 0.3 μm normalized transverse emittance and 200 keV energy spread (Table 1). While transporting the usual, kA-scale beam from the LCLS-II linac through the 2 km SLAC bypass line is challenging due to collective beam instabilities, the low, 100 A-scale current required for the XFELO is expected to be feasible.

To verify this, *ELEGANT* simulations [10] were carried out starting with the LCLS-II at the BSY and transporting through using the existing optics model to ESA and include wake effects, CSR and ISR. As is found for the usual LCLS-II case, there is an electron beam energy chirp not cancelled by the transport wakes. We therefore presume a passive, parallel-plate corrugated dechirper [11] like the one being considered for the nominal LCLS-II can be employed to remove the correlated energy spread. Simulations then largely confirm that the beam can be delivered to ESA while still satisfying the parameters of Table 1, with the final longitudinal *t-E* phase space shown in Figure 3. However, as seen in Figure 3, nonlinear wakes result in only ~200 fs of useful beam current that may reduce the available on-energy FEL gain suggesting additional room for improvement.

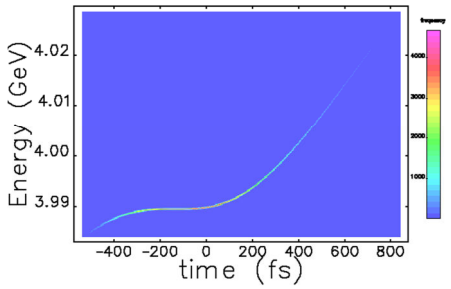

Figure 3: *ELEGANT* simulation of longitudinal phase space after beam transport to ESA

ESTIMATED PERFORMANCE

To make a preliminary estimate of steady-state performance, we now consider the single-pass cavity gains and losses. For starters, the high-reflectivity, few to tens meV-bandwidth Bragg reflectors demonstrated in [6] are presumed. Nominally these will result in a 1% loss per crystal with the thin out-coupling crystal additionally transmitting 4% of the intracavity power.

To estimate loss on the cylindrically symmetric CRLs, we consider X-ray absorption through the geometry shown in Figure 4. Assuming a Gaussian intensity profile incident on the CRLs, we find that the resulting absorption loss $L_{CRL} = 1 - P_{transmitted} / P_{incident}$ is given by

$$L_{CRL} = 1 - \frac{\sigma_{eff}^2}{\sigma^2} \exp(-d / l_{abs}), \qquad (1)$$

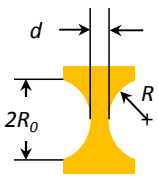

Figure 4: Cross sectional geometry of CRL

where l_{abs} is the material attenuation coefficient and σ_{eff} is the effective transmitted spot size

$$\sigma_{eff} = \left(\frac{1}{\sigma^2} + \frac{2}{R l_{abs}} \right)^{-1/2}, \quad (2)$$

with σ the incident RMS X-ray spot size. Assuming beryllium CRLs and σ = 30 μm, we arrive at a loss of 0.26% - 0.44% per CRL, depending on the grade of Be used. The very low estimate is largely due to the small spot size incident on the CRLs.

Combining 1% loss for each of 4 CRLs (assuming CRL pairs will be needed to achieve the 20 m focal length required), 1% loss on 3 Bragg crystals, and 5% loss on the out-coupling crystal, we therefore expect 11.5% loss per pass which we regard as 15% for good measure.

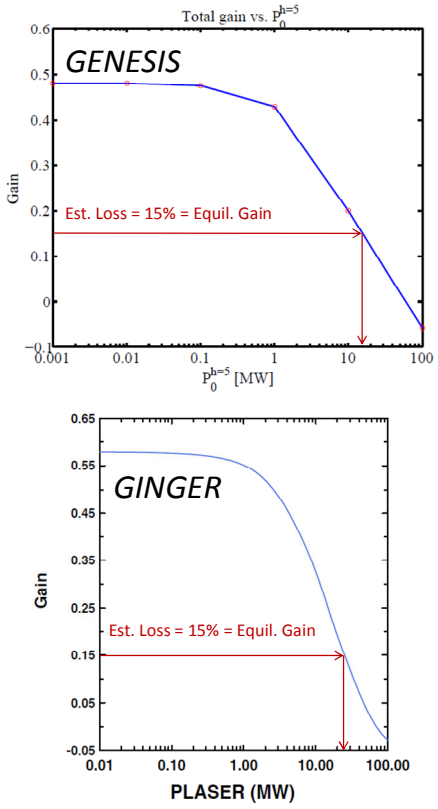

Figure 5: *GENESIS* and *GINGER* simulations of 1-pass power gain as a function of the intracavity X-ray power

To verify the analytically estimated 40.8% per-pass gain and to establish the steady-state equilibrium intracavity power, simplified 2D (*GINGER* [12]) and 3D (*GENESIS* [13]) fifth harmonic, seeded FEL simulations were performed assuming an ideal Gaussian bunch with the parameters shown in Table 1. The seed energy (representing the recirculating intracavity power) is scanned from zero to many MW and the percentage gain of a single pass is recorded, as shown in Figure 5. Start-up gain is ~50%, exceeding the low-gain estimate as higher-order gain is also found to contribute. As cavity power increases, per-pass amplification saturates and the gain drops. Then with the expected loss of 15% per pass, from Figure 5 we estimate an equilibrium peak power of ~20 MW, 0.8 MW of which is coupled out of the cavity.

From more recent, rigorous simulations of a similar proposed XFELO [5] as well as [8], the expected output bandwidth is ~5 meV after XFELO gain narrowing, and with pulse duration ~400 fs FWHM. This suggests the 0.8 MW output power is delivered in Fourier-limited, 0.33 μJ pulses at the ~2 MHz repetition rate, or spectral flux of 6×10^{13} ph./s/meV. This result is at least two orders greater than the best $10^{(9\text{ to }11)}$ ph./s/meV reported by synchrotron-based inelastic X-ray scattering beamlines. Output is well into hard X-ray energies (14.4 keV) utilizing the LCLS-II baseline energy of 4 GeV. Furthermore, output is found to be ~50 times greater average flux and 3-4 orders of magnitude higher average spectral flux (per meV) than estimates of (non-Fourier limited) nonlinear LCLS-II third harmonic gain at 14.4 keV [14].

CONCLUSION

We conclude that the proposed XFELO is indeed feasible and with significant improvement over established X-ray generation techniques. Work remains in precise optimization of the electron beam to feed into start-to-end XFELO modelling, for which the code *GINGER* has been modified to allow many-pass, fifth harmonic XFELO simulations. Additionally, other X-ray cavity-based FEL schemes remain for serious consideration including the regeneratively amplified FEL (RAFEL), once considered for the LCLS [15], as well as schemes fitting the footprint of the presently proposed LCLS-II undulator hall.

These cavity-based methods provide a potential avenue towards FELs with the stability and precision offered by now-conventional, mode-locked optical oscillators. Effort is ongoing in the development of component X-ray optics and optomechanics common to the construction of any such X-ray cavity. This includes evaluation of high-reflectivity Bragg crystal and high-transmission CRL performance under high average power, as well as the wavefront preservation and small-angle X-ray scattering losses in the CRLs. Also, to satisfy the nrad pointing stability required to recirculate the micrometer-scale wavefront over tens of meters, ultra-precise crystal movers [16] and active feedback [17] are also under investigation.

Once these components can be assembled into a realistic scale X-ray cavity, a new generation of ultra-stable, ultra-bright light sources can be realized when coupled with advanced, CW accelerators such as the future LCLS-II.

ACKNOWLEDGEMENTS

We would like to thank Tor Raubenheimer, Paul Emma, and Dieter Walz of SLAC for fruitful discussions and support.

REFERENCES

[1] P. Emma, *et al.*, "First lasing and operation of an ångstrom-wavelength free-electron laser," Nature Photonics **4**, 641 (2010).

[2] T. Ishikawa, *et al.*, "A compact X-ray free-electron laser emitting in the sub-ångstrom region," Nature Photonics **6**, 540 (2012).

[3] J. Amann, *et al.*, "Demonstration of self-seeding in a hard-X-ray free-electron laser," Nature Photonics **6**, 693 (2012).

[4] SLAC National Accelerator Laboratory, *Linac Coherent Light Source II Conceptual Design Report*, No. SLAC-R-978 (2011).

[5] K.-J. Kim, Y. Shvyd'ko, and Sven Reiche, "A Proposal for an X-Ray Free-Electron Laser Oscillator with an Energy-Recovery Linac," Phys. Rev. Lett. **100**, 244802 (2008).

[6] Y. Shvyd'ko, S. Stoupin, V. Blank, and S. Terentyev, "Near-100% Bragg reflectivity of X-rays," Nature Photonics **5**, 539 (2011).

[7] K.-J. Kim and Y. V. Shvyd'ko, "Tunable optical cavity for an x-ray free-electron-laser oscillator," Phys. Rev. ST Accel. Beams **12**, 030703 (2009).

[8] J. Dai, H. Deng, and Z. Dai, "Proposal for an X-Ray Free Electron Laser Oscillator with Intermediate Energy Electron Beam," Phys. Rev. ST Accel. Beams **108**, 034802 (2012).

[9] K.-J. Kim, "FEL gain taking into account diffraction and electron beam emittance; generalized Madey's theorem," Nucl. Instrum. Meth. A **318**, 489 (1992).

[10] M. Borland, "Elegant: A flexible SDDS-Compliant Code for Accelerator Simulation," Advanced Photon Source Report No. LS-287 (2000).

[11] Z. Zhang, *et al.*, "Electron beam energy chirp control with a rectangular corrugated structure at the Linac Coherent Light Source," Phys. Rev. ST Accel. Beams **18**, 010702 (2015).

[12] W. M. Fawley, "A User Manual for GINGER and its Post-Processor XPLOTGIN," SLAC LCLS Technical Note, No. LCLS-TN-04-03 (2004).

[13] S. Reiche, *et al.*, "GENESIS 1.3: a fully 3D time-dependent FEL simulation code," Nucl. Instrum. Meth. A **429**, 243 (1999).

[14] G. Marcus and T. Raubenheimer, "LCLS-II Hard X-Ray Undulator Harmonics," SLAC LCLS-II Technical Note, No. TN-15-11 (2015).

[15] Z. Huang and R.D. Ruth, "Fully Coherent X-Ray Pulses from a Regenerative-Amplifier Free-Electron Laser," Phys. Rev. Lett. **96**, 144801 (2006).

[16] D. Shu, *et al.*, "Development and applications of a two-dimensional tip-tilting stage system with nanoradian-level positioning resolution," Nucl. Instrum. Meth. A **649**, 114 (2011).

[17] S. Stoupin, *et al.*, "Nanoradian angular stabilization of x-ray optical components," Rev. Sci. Instrum. **81**, 055108 (2010).

[18] Z. Huang and K.-J. Kim, "Review of x-ray free-electron laser theory," Phys. Rev. ST Accel. Beams **10**, 034801 (2007).